MICROPOROUS NETWORKS

Pore chemistry and size control in hybrid porous materials for acetylene capture from ethylene

Xili Cui,[1]* Kaijie Chen,[2]* Huabin Xing,[1]† Qiwei Yang,[1] Rajamani Krishna,[3] Zongbi Bao,[1] Hui Wu,[4] Wei Zhou,[4] Xinglong Dong,[5] Yu Han,[5] Bin Li,[6] Qilong Ren,[1] Michael J. Zaworotko,[2]† Banglin Chen[6]†

The trade-off between physical adsorption capacity and selectivity of porous materials is a major barrier for efficient gas separation and purification through physisorption. We report control over pore chemistry and size in metal coordination networks with hexafluorosilicate and organic linkers for the purpose of preferential binding and orderly assembly of acetylene molecules through cooperative host-guest and/or guest-guest interactions. The specific binding sites for acetylene are validated by modeling and neutron powder diffraction studies. The energies associated with these binding interactions afford high adsorption capacity (2.1 millimoles per gram at 0.025 bar) and selectivity (39.7 to 44.8) for acetylene at ambient conditions. Their efficiency for the separation of acetylene/ethylene mixtures is demonstrated by experimental breakthrough curves (0.73 millimoles per gram from a 1/99 mixture).

An urgent demand for efficient solutions to challenges in gas separation, sensing, and storage (*1*–*7*) has spurred research on custom-designed porous materials, termed metal-organic frameworks (MOFs) and/or porous coordination polymers (PCPs) (*8*), in which open lattices are formed from inorganic centers (nodes) and organic linking groups. These materials can be designed from first principles and, thanks to their inherent diversity, afford precise control over pore chemistry and pore size.

Ideal porous materials for gas separation should exhibit high selectivity and optimal adsorption capacity for the target gas molecules at relevant conditions. However, the design of new materials that improve upon existing benchmarks poses a daunting challenge to materials scientists (*9*–*12*). For example, porous materials are needed for acetylene (C_2H_2) capture and separation from ethylene (C_2H_4) (*13*–*17*), industrial processes that are relevant for the production of polymer-grade C_2H_2 and C_2H_4 (the most produced organic compound in the world, at over 140 million metric tons in 2014). The MOF-74 family of compounds has a high density of open metal sites that drive high uptake of C_2H_2 but displays low separation selectivities (*18*). The M′MOF (mixed metal–organic framework) family has ultramicropores that enable sieving effects and high separation selectivities but relatively low uptake of C_2H_2 (*19*).

We report that metal coordination networks with preformed inorganic and organic linkers—SIFSIX-2-Cu-i [SIFSIX, hexafluorosilicate (SiF_6^{2-}); 2, 4,4′-dipyridylacetylene; i, interpenetrated)] (*20*) and SIFSIX-1-Cu (1, 4,4′-bipyridine) (*21*)—can exhibit exceptional C_2H_2 capture performance because the geometric disposition of SiF_6^{2-} moieties enables preferential binding of C_2H_2 molecules. Both materials have pore spaces that enable extremely high C_2H_2 capture under low pressures, and they unexpectedly represent new benchmarks for the highly efficient removal of minor amounts of C_2H_2 from C_2H_4 gas (SIFSIX-2-Cu-i) and mass separation of C_2H_2/C_2H_4 mixtures under ambient conditions (SIFSIX-1-Cu). We attribute this unprecedented performance to the existence of "sweet spots" in pore chemistry and pore size that enable highly specific recognition and high uptake of C_2H_2 to occur in the same material.

In these SIFSIX materials, two-dimensional (2D) nets of organic ligand and metal node are pillared with SiF_6^- anions in the third dimension to form 3D coordination networks that have primitive cubic topology and, importantly, pore walls lined by inorganic anions (*20*–*23*). The pore sizes within this family of materials can be systematically tuned by changing the length of the organic linkers, the metal node, and/or the framework interpenetration. SIFSIX-1-Cu, SIFSIX-2-Cu, SIFSIX-2-Cu-i, SIFSIX-3-Cu (3, pyrazine), SIFSIX-3-Zn, and SIFSIX-3-Ni have already been studied for their exceptional CO_2 capture performance, but here we report a study of their C_2H_2 and C_2H_4 adsorption from 283 to 303 K. Figure 1, A and B, and figs. S2 to S7 show dramatically different adsorption behaviors for C_2H_2 than those observed for CO_2 (figs. S8 and S9) (*24*). SIFSIX-2-Cu-i rapidly adsorbs C_2H_2 at very low pressure (≤0.05 bar). Its C_2H_2 uptake reaches 2.1 mmol/g at 298 K and 0.025 bar (Fig. 1B), compared with an uptake of 1.78 mmol/g by UTSA-100a (*17*). This performance at low pressure indicates that SIFSIX-2-Cu-i has promise for capturing C_2H_2 when it is a minor component in a gas mixture. SIFSIX-1-Cu exhibits exceptionally high C_2H_2 uptake (8.5 mmol/g) at 298 K and 1.0 bar. This is not only the highest uptake of any of the SIFSIX materials, but is also even higher than that of the previous benchmark, FeMOF-74 (table S1) (*18*, *24*). As detailed herein, we attribute the unprecedented performance of these materials to their hybrid pore chemistry and optimal pore sizes for binding C_2H_2.

To understand the C_2H_2 adsorption isotherms in these materials, we conducted detailed modeling studies using first-principles DFT-D (dispersion-corrected density functional theory) calculations. In SIFSIX-1-Cu, C_2H_2 molecules are bound through strong C–H···F hydrogen (H) bonding (2.017 Å) and van der Waals (vdW) interactions with the 4,4′-bipyridine linkers (Fig. 1C and fig. S10) (*24*). The DFT-D–calculated static adsorption energy (ΔE) is 44.6 kJ/mol. Each unit cell of SIFSIX-1-Cu contains four equivalent exposed F atoms, and each exposed F atom binds one C_2H_2 molecule. The distance between neighboring adsorbed C_2H_2 molecules is ideal for them to synergistically interact with each other through multiple $H^{\delta+}\cdots C^{\delta-}$ dipole-dipole interactions (Fig. 1C), further enhancing the energy of adsorption. Because four C_2H_2 molecules are adsorbed per unit cell, the ΔE of C_2H_2 increases to 47.0 kJ/mol. The strong binding of C_2H_2 at F atoms and the geometric arrangement of SiF_6^{2-} anions enable the efficient packing of four C_2H_2 molecules per unit cell and very high C_2H_2 uptake at 298 K and 1.0 bar (about 4.4 C_2H_2 molecules per unit cell).

C_2H_2 adsorption is weaker in the wider-pore material SIFSIX-2-Cu (10.5 Å × 10.5 Å cavity) than in SIFSIX-1-Cu (ΔE, 34.6 versus 44.6 kJ/mol; uptake, 5.3 versus 8.5 mmol/g). The C–H···F H-bonding interaction from SiF_6^{2-} sites is of the same nature in these isoreticular networks (Fig. 1, C and D). However, the vdW interaction between C_2H_2 and the organic linker in SIFSIX-2-Cu is weak compared with that in SIFSIX-1-Cu. We attribute this difference to the former's larger pore size and weaker vdW potential overlap (figs. S10 and S11) (*24*). Moreover, at high gas uptake, the C_2H_2 molecules adsorbed on adjacent F sites are too far separated to have synergistic guest-guest interactions. However, in the twofold interpenetrated structure of SIFSIX-2-Cu-i, one C_2H_2 molecule can be simultaneously bound by two F atoms from different nets through cooperative C–H···F H-bonding (2.013 and 2.015 Å; Fig. 1E), which enables the strongest energy of C_2H_2 binding yet observed in SIFSIX materials (ΔE, 52.9 kJ/mol). The strong adsorption energy of SIFSIX-2-Cu-i contributes to its extremely high uptake capacity at low pressure. In SIFSIX-3-Zn and SIFSIX-3-Ni, which are

[1]Key Laboratory of Biomass Chemical Engineering of Ministry of Education, College of Chemical and Biological Engineering, Zhejiang University, Hangzhou 310027, China. [2]Department of Chemical and Environmental Sciences, University of Limerick, Limerick, Republic of Ireland. [3]Van 't Hoff Institute for Molecular Sciences, University of Amsterdam, Science Park 904, 1098 XH Amsterdam, Netherlands. [4]Center for Neutron Research, National Institute of Standards and Technology, Gaithersburg, MD 20899-6102, USA. [5]Advanced Membranes and Porous Materials Center, Physical Sciences and Engineering Division, King Abdullah University of Science and Technology, Thuwal 23955-6900, Saudi Arabia. [6]Department of Chemistry, University of Texas–San Antonio, One UTSA Circle, San Antonio, TX 78249-0698, USA.

*These authors contributed equally to this work. †Corresponding author. Email: xinghb@zju.edu.cn (H.X.); michael.zaworotko@ul.ie (M.J.Z.); banglin.chen@utsa.edu (B.C.)

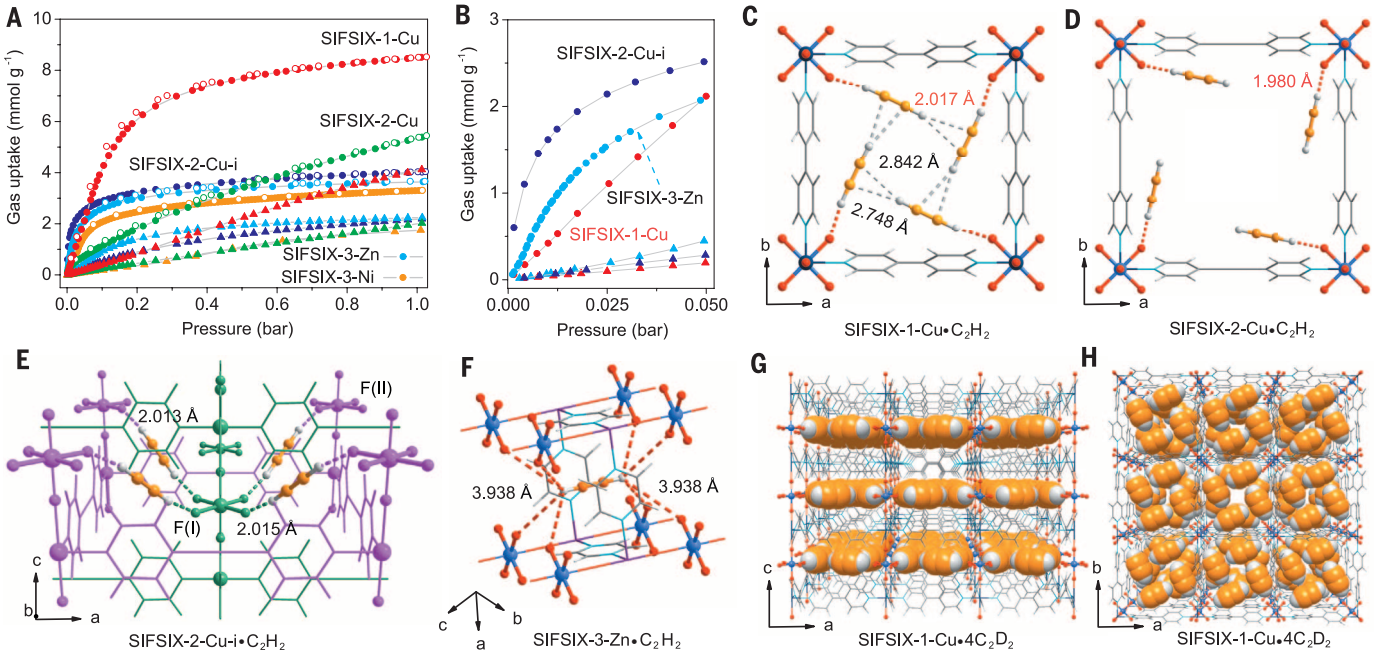

Fig. 1. C_2H_2 and C_2H_4 adsorption isotherms of the MOFs, DFT-D–simulated optimized C_2H_2 adsorption sites of the MOFs, and neutron crystal structure of SIFSIX-1-Cu·4C_2D_2. (**A** and **B**) Adsorption isotherms of C_2H_2 (filled circles) and C_2H_4 (triangles) in SIFSIX-1-Cu (red), SIFSIX-2-Cu (green), SIFSIX-2-Cu-i (blue), SIFSIX-3-Zn (light blue), and SIFSIX-3-Ni (orange) at 298 K in two pressure regions, 0 to 1.0 bar (A) and 0 to 0.05 bar (B). Open circles in (A) are desorption isotherms of C_2H_2 (**C** to **F**) DFT-D–calculated C_2H_2 adsorption binding sites in SIFSIX-1-Cu (C), SIFSIX-2-Cu (D), SIFSIX-2-Cu-i (E) (the different nets are highlighted in magenta and green for clarity), and SIFSIX-3-Zn (F). Color code: F, red; Si, light blue; C, gray; H, light gray; N, sky blue; Cu, dark teal; Zn, violet; C (in C_2H_2 or C_2D_2), orange. (**G** and **H**) Neutron crystal structure of SIFSIX-1-Cu·4C_2D_2 at 200 K, determined from Rietveld analysis.

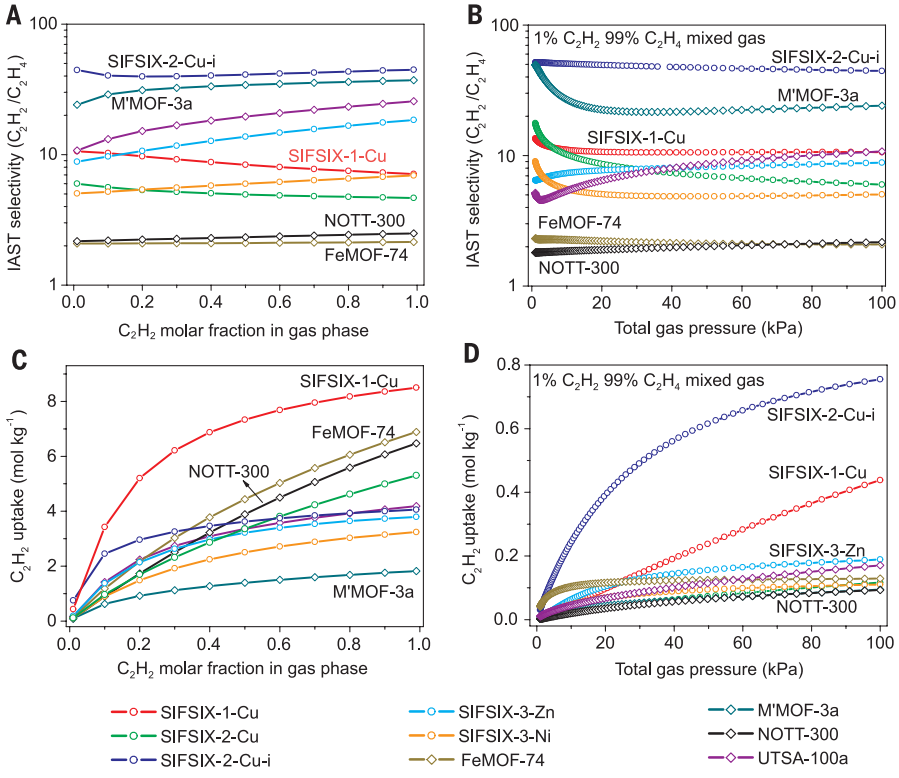

Fig. 2. IAST calculations for MOF performance with C_2H_2/C_2H_4 mixtures. (**A** and **B**) Comparison of the IAST selectivities of SIFSIX materials versus those of previously reported best-performing materials for C_2H_2/C_2H_4 mixtures. Results for varying C_2H_2 molar fractions at 100 kPa are shown in (A), and results at varying pressures for a 1% C_2H_2 mixture are shown in (B). (**C** and **D**) MOF capacity to uptake C_2H_2 from C_2H_2/C_2H_4 mixtures. Results for varying C_2H_2 molar fractions at 100 kPa are shown in (C), and results at varying pressures for a 1% C_2H_2 mixture are shown in (D).

the strongest CO_2 adsorbents, the pore size is smallest, and C_2H_2 molecules are primarily adsorbed at a different site in the 1D channel along the *c* axis (ΔE, 50.3 kJ/mol; Fig. 1F). The secondary adsorption site in SIFSIX-3-Zn (fig. S12) (*24*) exhibits a much smaller adsorption energy (25.9 kJ/mol), which results in lower C_2H_2 uptake compared with that of SIFSIX-2-Cu-i.

The weakly basic nature of the SiF_6^{2-} sites (acid dissociation constant pK_a, 1.92) and their geometric disposition enable strong binding with weakly acidic C_2H_2 molecules. Because C_2H_2 is more acidic than C_2H_4 (pK_a, 25 versus 44) (*17*), and the geometry of the SIFSIX materials is more optimal for C_2H_2 binding, there are much stronger interactions with C_2H_2 than with C_2H_4 (ΔE in SIFSIX-1-Cu, 44.6 versus 27.2 kJ/mol; ΔE in SIFSIX-2-Cu-i, 52.9 versus 39.8 kJ/mol). The calculated H-bond distances between C_2H_4 and SiF_6^{2-} sites are 2.541 and 2.186 Å in SIFSIX-1-Cu and SIFSIX-2-Cu-i, respectively, which are longer than those between C_2H_2 and SiF_6^{2-} sites (figs. S13 and S14) (*24*).

To establish the structure of the C_2H_2 binding sites through Rietveld structural refinements, high-resolution neutron powder diffraction data were collected on C_2D_2-loaded samples of SIFSIX-1-Cu·4C_2D_2 and SIFSIX-2-Cu-i·1.7C_2D_2 at 200 K (figs. S15 and S16) (*24*). Each unit cell of SIFSIX-1-Cu is filled with four C_2D_2 molecules that are arranged in an ordered planar structure (Fig. 1, G and H), consistent with the DFT-D modeling results. C–D···F H-bonding occurs between C_2D_2 and SiF_6^- anions (2.063 Å), and $D^{\delta+}\cdots C^{\delta-}$ distances between neighboring C_2D_2 molecules are 3.063 and 3.128 Å. In SIFSIX-2-Cu-i, each C_2H_2

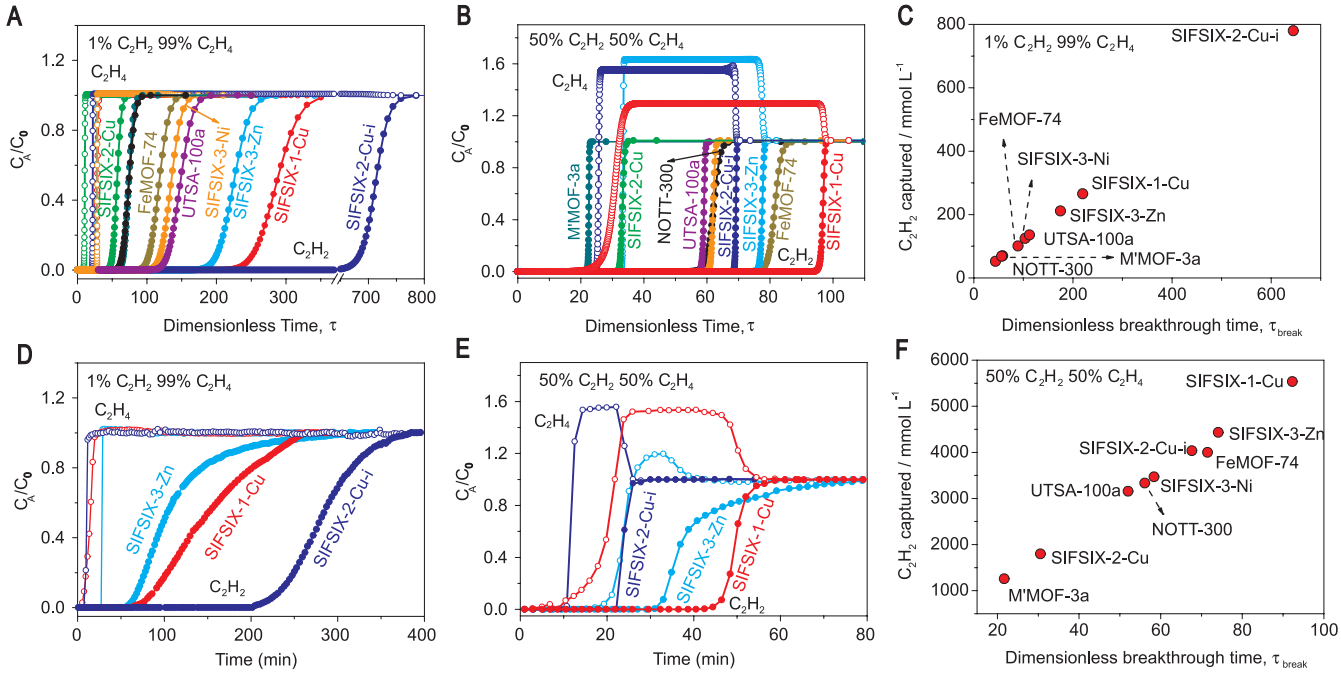

Fig. 3. Simulated and experimental column breakthrough results. (**A** and **B**) Simulated column breakthrough curves for C_2H_2/C_2H_4 separations with SIFSIX materials and previously reported best-performing materials [(A), 1/99 mixture; (B), 50/50 mixture]. (**C** and **F**) Plots of the amount of C_2H_2 captured as a function of τ_{break} in the simulated column breakthrough [(C), 1/99 mixture; (F), 50/50 mixture]. (**D** and **E**) Experimental column breakthrough curves for C_2H_2/C_2H_4 separations with SIFSIX-1-Cu, SIFSIX-2-Cu, and SIFSIX-3-Zn at 298 K and 1.01 bar [(D), 1/99 mixture; (E), 50/50 mixture]. In (A), (B), (D), and (E), open circles are for C_2H_4, and filled circles are for C_2H_2. C_A/C_0, outlet concentration/feed concentration.

interacts with two SiF_6^- anions via dual C–D···F H-bonding (2.134 Å; fig. S17) (*24*).

The separation of C_2H_2 from C_2H_4 is necessary for the production of high-purity C_2H_4 and C_2H_2. In the production of polymer-grade C_2H_4, removal of trace C_2H_2 (about 1%) from C_2H_4 gas must meet the requirement of <40 parts per million (ppm) C_2H_2 in the downstream polymerization reaction (*17*). Similarly, in the production of polymer-grade C_2H_2 by pyrolysis of coal and biomass, the capture of C_2H_2 from C_2H_2/C_2H_4 mixtures (90/10 to 50/50, v/v) is a crucial step. Existing methods, such as solvent absorption and partial hydrogenation of C_2H_2 (*25*), are energy intensive, so there is an urgent need to develop efficient porous materials for C_2H_2 capture from C_2H_4.

To address gas mixture separations, we first determined the C_2H_2/C_2H_4 separation selectivities of the SIFSIX materials by means of ideal adsorbed solution theory (IAST) calculations (Fig. 2 and fig. S20) (*24*, *26*). SIFSIX-2-Cu-i exhibits record C_2H_2/C_2H_4 selectivities (39.7 to 44.8; Fig. 2A), even greater than those of M'MOF-3a (table S1). Because SIFSIX-2-Cu-i adsorbs a high amount of C_2H_2 under very low pressures, it not only has the highest C_2H_2/C_2H_4 selectivities (Fig. 2B) but also the highest C_2H_2 uptake (Fig. 2D) for C_2H_2/C_2H_4 (1/99) mixtures. SIFSIX-1-Cu displays moderately high C_2H_2/C_2H_4 separation selectivities (7.1 to 10.6), which are greater than those of FeMOF-74 (2.1) (*18*) and NOTT-300 (2.2 to 2.5) (*14*) (Fig. 2A). For C_2H_2/C_2H_4 (1/99) mixtures, SIFSIX-1-Cu exhibits greater selectivities (10.6) than SIFSIX-3-Zn (8.8) and SIFSIX-3-Ni (5.0) (Fig. 2B). Its C_2H_2 uptake from the 1/99 mixture is the second highest of the compounds investigated (Fig. 2D). Given that SIFSIX-1-Cu has a relatively large surface area, it should also be very efficient for C_2H_2/C_2H_4 (1/99) separation. SIFSIX-1-Cu exhibits higher C_2H_2 uptakes than benchmark MOFs, including FeMOF-74, NOTT-300, and UTSA-100a. Its high C_2H_2/C_2H_4 selectivities (Fig. 2A) make SIFSIX-1-Cu most suitable for C_2H_2/C_2H_4 (50/50) separation (Fig. 2C and fig. S20) (*24*). Some further comparisons of how these MOFs perform with respect to C_2H_2/C_2H_4 separations are shown in table S1 (*24*).

Transient breakthrough simulations (*27*) were conducted to demonstrate the C_2H_2/C_2H_4 separation performances of the SIFSIX materials in column adsorption processes. Two C_2H_2/C_2H_4 mixtures (1/99 and 50/50) were used as feeds to mimic the industrial process conditions. Clean separations were realized with all five SIFSIX MOFs; C_2H_4 first eluted through the bed to yield a polymer-grade gas, then C_2H_2 broke through from the bed at a certain time τ_{break} (Fig. 3A and figs. S21 and S22) (*24*). The dimensionless τ_{break} values for SIFSIX-1-Cu (1/99 and 50/50 mixtures) and SIFSIX-2-Cu-i (1/99 mixture) exceed those of the other SIFSIX materials and MOFs that we studied (Fig. 3, A and B). The amount of C_2H_2 captured from the 1/99 mixture in SIFSIX-1-Cu and SIFSIX-2-Cu-i was as high as 265.3 and 780.0 mmol/liter, respectively, which compares favorably with state-of-art adsorbents such as UTSA-100a (135.5 mmol/liter), FeMOF-74 (100.7 mmol/liter), and NOTT-300 (68.3 mmol/liter). SIFSIX-2-Cu-i efficiently removes trace C_2H_2 from C_2H_4 gas (1/99 mixture), whereas SIFSIX-1-Cu demonstrates excellent C_2H_2 capacity with an uptake of 5533 mmol/liter from the 50/50 mixture, ~37% greater than that of FeMOF-74 (Fig. 3F).

Through experimental breakthrough studies, we further examined these materials in actual adsorption processes for both 1/99 and 50/50 mixtures. Highly efficient separations for C_2H_2/C_2H_4 mixtures were realized (Fig. 3, D and E). For the capture of C_2H_2 from the 1/99 mixture, the concentration of C_2H_2 in the gas exiting the adsorber for up to 140 min was below 2 ppm, and the purity of C_2H_4 was >99.998% (fig. S23) (*24*). The hierarchy of breakthrough times for the 1/99 mixture was, from longest to shortest, SIFSIX-2-Cu-i, SIFSIX-1-Cu, then SIFSIX-3-Zn; for the 50/50 mixture, it was SIFSIX-1-Cu, SIFSIX-3-Zn, then SIFSIX-2-Cu-i (Fig. 3, D and E). These experiments are consistent with simulated breakthrough results. Although the uptake of C_2H_2 by SIFSIX-3-Zn at low pressure for the 1/99 mixture is higher than that by SIFSIX-1-Cu (Fig. 1B), SIFSIX-1-Cu exhibits a longer breakthrough time for C_2H_2, presumably because of its higher selectivity (Fig. 2B). The amounts of C_2H_2 captured by SIFSIX-1-Cu, SIFSIX-2-Cu-i, and SIFSIX-3-Zn from the 1/99 mixture (0.38, 0.73, and 0.08 mmol/g, respectively) and from the 50/50 mixture (6.37, 2.88, and 1.52 mmol/g, respectively) during the breakthrough process are in excellent agreement with the simulated results, except in the case of SIFSIX-3-Zn (tables S12 and S13) (*24*).

In the production of high-purity C_2H_4, the feed gases for the C_2H_2 removal unit are contaminated with trace levels of CO_2 (<50 ppm), H_2O (<5 ppm), and O_2 (<5 ppm). We conducted breakthrough experiments for the 1/99 mixture with SIFSIX-2-Cu-i, the best-performing material for capturing trace

amounts of C_2H_2. These experiments indicate that the presence of CO_2 has only a slight (1000 ppm CO_2) or no (10 ppm CO_2) effect on the separation of C_2H_2 from C_2H_4 (fig. S24) (*24*). Moisture (6 to 1340 ppm) and oxygen (2200 ppm) do not affect the C_2H_2 capture ability of SIFSIX-2-Cu-i (figs. S25 and S26) (*24*). The breakthrough performances of SIFSIX-2-Cu-i and SIFSIX-3-Zn for the 1/99 mixture did not decline during 16 and 3 cycles, respectively (figs. S28 and S29) (*24*), and the SIFSIX materials retained their stability after breakthrough experiments (figs. S1 and S30) (*24*).

The SIFSIX materials that we studied exhibit excellent C_2H_2 storage performance. The volumetric uptake of C_2H_2 by SIFSIX-1-Cu at 298 K and 1.0 bar is the highest among these SIFSIX materials (0.191 g/cm^3; table S14) (*24*). The C_2H_2 storage densities in the pores of SIFSIX-1-Cu, SIFSIX-2-Cu-i, and SIFSIX-3-Zn at 298 K are 0.388, 0.403, and 0.499 g/cm^3, respectively.

The basic principles outlined here are likely to be applicable to other gas mixtures. Primary binding sites will be necessary for recognition of specific gas molecules, whereas suitable pore sizes and spacing will be needed to enforce synergistic binding to multiple sites in order to form the so-called "gas clusters" through intermolecular guest-guest interactions. This work not only reveals a path forward for industrial C_2H_2/C_2H_4 separations, but also facilitates a design or crystal engineering approach to the development of porous materials for other gas separations.

REFERENCES AND NOTES

1. S. Kitagawa, *Angew. Chem. Int. Ed.* **54**, 10686–10687 (2015).
2. R. Vaidhyanathan *et al.*, *Science* **330**, 650–653 (2010).
3. N. T. T. Nguyen *et al.*, *Angew. Chem. Int. Ed.* **53**, 10645–10648 (2014).
4. N. L. Rosi *et al.*, *Science* **300**, 1127–1129 (2003).
5. Y. Peng *et al.*, *J. Am. Chem. Soc.* **135**, 11887–11894 (2013).
6. J. A. Mason *et al.*, *Nature* **527**, 357–361 (2015).
7. S. Ma *et al.*, *J. Am. Chem. Soc.* **130**, 1012–1016 (2008).
8. H. Furukawa, K. E. Cordova, M. O'Keeffe, O. M. Yaghi, *Science* **341**, 1230444 (2013).
9. S. J. Datta *et al.*, *Science* **350**, 302–306 (2015).
10. Z. J. Zhang, Z.-Z. Yao, S. Xiang, B. Chen, *Energy Environ. Sci.* **7**, 2868–2899 (2014).
11. Q. Lin, T. Wu, S. T. Zheng, X. Bu, P. Feng, *J. Am. Chem. Soc.* **134**, 784–787 (2012).
12. J.-R. Li, R. J. Kuppler, H.-C. Zhou, *Chem. Soc. Rev.* **38**, 1477–1504 (2009).
13. R. Matsuda *et al.*, *Nature* **436**, 238–241 (2005).
14. S. Yang *et al.*, *Nat. Chem.* **7**, 121–129 (2014).
15. H. Wu, Q. Gong, D. H. Olson, J. Li, *Chem. Rev.* **112**, 836–868 (2012).
16. J.-P. Zhang, X.-M. Chen, *J. Am. Chem. Soc.* **131**, 5516–5521 (2009).
17. T. L. Hu *et al.*, *Nat. Commun.* **6**, 7328–7335 (2015).
18. E. D. Bloch *et al.*, *Science* **335**, 1606–1610 (2012).
19. M. C. Das *et al.*, *J. Am. Chem. Soc.* **134**, 8703–8710 (2012).
20. P. Nugent *et al.*, *Nature* **495**, 80–84 (2013).
21. S. Noro *et al.*, *J. Am. Chem. Soc.* **124**, 2568–2583 (2002).
22. O. Shekhah *et al.*, *Nat. Commun.* **5**, 4228–4234 (2014).
23. A. Kumar *et al.*, *Angew. Chem. Int. Ed.* **54**, 14372–14377 (2015).
24. Materials and methods are available as supplementary materials on *Science* Online.
25. F. Studt *et al.*, *Science* **320**, 1320–1322 (2008).
26. K. S. Walton, D. S. Sholl, *AIChE J.* **61**, 2757–2762 (2015).
27. R. Krishna, *RSC Adv.* **5**, 52269–52295 (2015).

ACKNOWLEDGMENTS

This work is supported by the National Natural Science Foundation of China (grants 21222601, 21436010, and 21476192), Zhejiang Provincial Natural Science Foundation of China (grant LR13B060001), Ten Thousand Talent Program of China (to H.X.), the Welch Foundation (grant AX-1730), King Abdullah Science and Technology University Office of Competitive Research Funds (grant URF/1/1672-01-01), and the Science Foundation Ireland (award 13/RP/B2549 to M.Z.). We thank T. L. Hu, Y. F. Zhao, W. D. Shan, and M. D. Jiang for their help and arrangement of the breakthrough experiments; A. Kumar for help with sample characterization; and Z. G. Zhang and B. G. Su for discussions of the experiments. Metrical data for the solid-state structures of SIFSIX-2-Cu-i·C_2D_2 and SIFSIX-1-Cu·C_2D_2 are available free of charge from the Cambridge Crystallographic Data Centre under reference numbers CCDC 1471795 and 1471796.

The authors and their affiliated institutions have filed a patent application related to the results presented here.

SUPPLEMENTARY MATERIALS

www.sciencemag.org/content/353/6295/141/suppl/DC1
Materials and Methods
Figs. S1 to S32
Tables S1 to S15
References (*28*–*34*)

12 January 2016; accepted 5 May 2016
Published online 19 May 2016
10.1126/science.aaf2458

ORGANIC CHEMISTRY

Copper-catalyzed asymmetric addition of olefin-derived nucleophiles to ketones

Yang Yang,[1] Ian B. Perry,[1] Gang Lu,[2] Peng Liu,[2]* Stephen L. Buchwald[1]*

Enantioenriched alcohols found in an array of bioactive natural products and pharmaceutical agents are often synthesized by asymmetric nucleophilic addition to carbonyls. However, this approach generally shows limited functional-group compatibility, requiring the use of preformed organometallic reagents in conjunction with a stoichiometric or substoichiometric amount of chiral controller to deliver optically active alcohols. Herein we report a copper-catalyzed strategy for the stereoselective nucleophilic addition of propargylic and other alkyl groups to ketones, using easily accessible (poly)unsaturated hydrocarbons as latent carbanion equivalents. Our method features the catalytic generation of highly enantioenriched organocopper intermediates and their subsequent diastereoselective addition to ketones, allowing for the effective construction of highly substituted stereochemical dyads with excellent stereocontrol. Moreover, this process is general, scalable, and occurs at ambient temperature.

Stereochemically complex alcohols in optically pure form are commonly encountered structural elements in a diverse range of pharmaceutical drugs and biologically active natural products (Fig. 1A). Consequently, general methods that allow for the stereoselective assembly of highly substituted alcohols have long been sought (*1*). The discovery of Grignard reagents and their subsequent addition to ketones and aldehydes have been widely considered as milestones in synthetic chemistry, giving rise to a general synthesis of alcohols from preformed organomagnesium reagents and broadly available carbonyl compounds (*2*). Since then, extensive efforts have been devoted to the development of asymmetric variants of nucleophilic addition reactions to carbonyls, using preformed organometallic reagents (*1*, *3*–*7*). These synthetic endeavors have proven to be exceptionally fruitful, culminating in a variety of protocols for enantioselective additions to carbonyls, using either a chiral auxiliary-modified organometallic reagent or a substoichiometric amount of chiral controller to achieve excellent levels of stereocontrol. Compared with aldehydes, however, the asymmetric nucleophilic addition to ketones has been studied to a lesser extent (*5*–*7*).

Although numerous advances have been made in this area, considerable hurdles have impeded the further adaptation of these methods by the synthetic community. The requirement to prepare and use a stoichiometric quantity of an organometallic reagent complicates most of the existing methods. In addition, the highly nucleophilic and basic nature of organometallic reagents has posed substantial limitations with respect to the functional-group compatibility of these processes. As a consequence, these methods are typically not amenable to the transformation of late-stage intermediates and other highly functionalized molecules. Furthermore, an additional synthetic operation is required to prepare these organometallic reagents from organic halide or unsaturated hydrocarbon precursors, imposing further constraints on the types of nucleophiles suitable for carbonyl addition.

In this context, a catalytic method for stereoselective additions to carbonyls, using easily accessible olefins as latent carbanion equivalents in

[1]Department of Chemistry, Massachusetts Institute of Technology (MIT), Cambridge, MA 02139, USA. [2]Department of Chemistry, University of Pittsburgh, Pittsburgh, PA 15260, USA.
*Corresponding author. Email: pengliu@pitt.edu (P.L.); sbuchwal@mit.edu (S.L.B.)

Editor's Summary

Separating one organic from another

Separating closely related organic molecules is a challenge (see the Perspective by Lin).The separation of acetylene from ethylene is needed in high-purity polymer production. Cui et al. developed a copper-based metal-organic framework with hexafluorosilicate and organic linkers designed to have a high affinity for acetylene. These materials, which capture four acetylene molecules in each pore, successfully separated acetylene from mixtures with ethylene. Propane and propylene are both important feedstock chemicals. Their physical and chemical similarity, however, requires energy-intense processes to separate them. Cadiau et al. designed a fluorinated porous metal-organic framework material that selectively adsorbed propylene, with the complete exclusion of propane.

Science, this issue pp. 141 and 137; see also p. 121